1999

Trajectory calculations for spherical geodesic grids in Cartesian space

Giraldo, F.X.

Monthly Weather Review / Volume 127, Issue 7, 1651-1662
http://hdl.handle.net/10945/25516

NOTES AND CORRESPONDENCE

Trajectory Calculations for Spherical Geodesic Grids in Cartesian Space

FRANCIS X. GIRALDO

Naval Research Laboratory, Monterey, California

9 April 1998 and 30 July 1998

ABSTRACT

This paper shows how to obtain accurate and efficient trajectory calculations for spherical geodesic grids in Cartesian space. Determination of the departure points is essential to characteristic-based methods that trace the value of a function to the foot of the characteristics and then either integrate or interpolate at this location. In this paper, the departure points are all computed in relation to the spherical geodesic grids that are composed of a disjoint set of unstructured equilateral triangles. Interpolating and noninterpolating trajectory calculation approaches are both illustrated and the accuracy of both methods are compared. The noninterpolating method of McGregor results in the most accurate trajectories. The challenge in using McGregor's method on unstructured triangular grids lies in the computation of the derivatives required in the high-order terms of the Taylor series expansion. This paper extends McGregor's method to unstructured triangular grids by describing an accurate and efficient method for constructing the derivatives in an element by element approach typical of finite element methods. An order of accuracy analysis reveals that these numerical derivatives are second-order accurate.

1. Introduction

The solution of partial differential equations on the sphere is of prime importance in meteorology and oceanography. The proper coordinate system would appear to be the spherical coordinates but this system poses some challenging problems at the poles not only for Eulerian formulations of the equations but for Lagrangian formulations as well. The pole problem can be overcome in a variety of ways, such as the use of Cartesian rather than spherical coordinates to write the differential equations. This approach was used in Giraldo (1997) for the advection equation. This approach may also be used for the shallow water equations by using the Lagrange multiplier formulation of Côté (1988). Côté writes the equations in Cartesian coordinates but then includes an extra forcing term obtained by using Lagrange multipliers. This forcing term constrains the motion of all fluid particles to remain on the sphere. We are very much interested in this formulation as we are currently developing a weak Lagrange–Galerkin shallow water model on the sphere using Cartesian coordinates [see Giraldo (1997) for details of the weak Lagrange–Galerkin method]. For this reason, this paper only deals with the determination of the departure points in Cartesian space.

Corresponding author address: Francis X. Giraldo, Naval Research Laboratory, 7 Grace Hopper Ave., Monterey, CA 93943.
E-mail: giraldo@nrlmry.navy.mil

McGregor (1993) introduced an economical departure point calculation procedure that does not involve interpolation. His scheme is very efficient and accurate but the implementation of the method was only illustrated for rectangular grids. This paper shows the implementation of McGregor's approach on unstructured triangular grids such as those composing the spherical geodesic grids.

2. Governing equation

Let us consider a simple equation for our study such that we have analytic values for the solution and the trajectories. In spherical coordinates the advection equation for the variable φ is

$$\frac{\partial \varphi}{\partial t} + \left[\frac{\tilde{u}}{a\cos\theta}\frac{\partial \varphi}{\partial \lambda} + \frac{\tilde{v}}{a}\frac{\partial \varphi}{\partial \theta}\right] + \left[\varphi\left(\frac{1}{a\cos\theta}\frac{\partial \tilde{u}}{\partial \lambda} + \frac{1}{a}\frac{\partial \tilde{v}}{\partial \theta} - \frac{\tilde{v}}{a}\tan\theta\right)\right] = 0, \quad (1)$$

where a is the radius of the sphere, $(\tilde{u}, \tilde{v})$ are the zonal and meridional velocity components, and (λ, θ) are the longitudinal and latitudinal coordinates. The first bracketed term represents the operator $\mathbf{u} \cdot \nabla\varphi$ and the second term represents $\varphi\nabla \cdot \mathbf{u}$. However, instead of using this form, let us look at the Cartesian form

$$\frac{\partial \varphi}{\partial t} + \left[u\frac{\partial \varphi}{\partial x} + v\frac{\partial \varphi}{\partial y} + w\frac{\partial \varphi}{\partial z}\right] + \left[\varphi\left(\frac{\partial u}{\partial x} + \frac{\partial v}{\partial y} + \frac{\partial w}{\partial z}\right)\right] = 0 \quad (2)$$

used in Giraldo (1997). This equation can now be written in the following compact form:

$$\frac{\partial \varphi}{\partial t} + \nabla \cdot (\mathbf{u}\varphi) = 0, \quad (3)$$

which is the conservation form of the advection equation where φ is some conservation variable, and $\mathbf{u}$ is the velocity vector. In Giraldo (1997), this equation was solved using the weak Lagrange–Galerkin method. Beginning with the method of weighted residuals with weight (i.e., basis) function ψ

$$\int_\Omega \psi\left[\frac{\partial \varphi}{\partial t} + \nabla \cdot (\mathbf{u}\varphi)\right] d\Omega = 0,$$

on domain Ω and integrating by parts such that

$$\psi\frac{\partial \varphi}{\partial t} = \frac{\partial \varphi\psi}{\partial t} - \varphi\frac{\partial \psi}{\partial t}$$

and

$$\psi\nabla \cdot (\mathbf{u}\varphi) = \nabla \cdot (\mathbf{u}\varphi\psi) - (\mathbf{u}\varphi) \cdot \nabla\psi,$$

we get

$$\int_\Omega \left[\frac{\partial \varphi\psi}{\partial t} + \nabla \cdot (\mathbf{u}\varphi\psi)\right] - \left[\varphi\left(\frac{\partial \psi}{\partial t} + \mathbf{u} \cdot \nabla\psi\right)\right] d\Omega = 0.$$

The basis functions ψ are chosen such that the second term in brackets disappears. In other words, the basis functions are chosen such that they are constant along the characteristics. This results in the simplified system

$$\int_\Omega \frac{\partial \varphi\psi}{\partial t} + \nabla \cdot (\mathbf{u}\varphi\psi)\, d\Omega = 0 \quad (4)$$

along with

$$\frac{\partial \psi}{\partial t} + \mathbf{u} \cdot \nabla\psi = 0$$

$$\frac{d\mathbf{x}}{dt} = \mathbf{u}(\mathbf{x}, t),$$

where

$$\frac{d}{dt} = \frac{\partial}{\partial t} + \mathbf{u} \cdot \nabla$$

denotes the total (or Lagrangian) derivative. By virtue of the Reynolds transport theorem, (4) now becomes

$$\frac{d}{dt}\int_\Omega \varphi\psi\, d\Omega = 0,$$

which, after integrating along the characteristics, gives

$$\int_{\Omega_A} \varphi(\mathbf{x}_A, t + \Delta t)\psi(\mathbf{x}_A, t + \Delta t)\, d\Omega_A = \int_{\Omega_D} \varphi(\mathbf{x}_D, t)\psi(\mathbf{x}_D, t)\, d\Omega_D, \quad (5)$$

where A and D denote arrival and departure points. [For further details on this method, refer to Giraldo (1997).] However, this is clearly not the only method of solving this equation using characteristic-based methods. In the case of a divergence-free flow, the Lagrangian form of (3) is

$$\frac{d\varphi}{dt} = 0 \quad (6)$$

$$\frac{d\mathbf{x}}{dt} = \mathbf{u}(\mathbf{x}, t). \quad (7)$$

Discretizing this equation by the semi-Lagrangian method and then applying the finite element method, yields the following relation:

$$\int_{\Omega_A} \varphi(\mathbf{x}_A, t + \Delta t)\psi(\mathbf{x}_A, t + \Delta t)\, d\Omega_A = \int_{\Omega_A} \varphi(\mathbf{x}_D, t)\psi(\mathbf{x}_A, t + \Delta t)\, d\Omega_A, \quad (8)$$

which is equivalent to

$$\varphi(\mathbf{x}_A, t + \Delta t) = \varphi(\mathbf{x}_D, t),$$

which is the typical semi-Lagrangian formulation for this equation regardless of which spatial discretization method we select. Note that the resulting equations for both methods are equivalent if and only if the flow is divergence free. The main difference between the two approaches is that (5) depends on integration while (8) on interpolation. The integration can be carried out exactly or by Gaussian quadrature. The interpolations, on the other hand, are a bit more complex on unstructured grids and perhaps the best approach is to use the kriging method described in Le Roux et al. (1997), although Lagrange interpolation on the triangles could certainly be used. However, the accuracy of both methods relies mainly on how accurate the trajectories are calculated; namely, how best to solve (7). The solution of this equation on unstructured triangular grids is the scope of this paper.

3. Test case

Numerical experiments are performed on the advection equation on the sphere, which is defined by (1). The initial condition is given as in Williamson et al. (1992) by the cosine wave

$$\varphi(\mathbf{x}, 0) = \begin{cases} \frac{h}{2}\left(1 + \cos\frac{\pi r}{R}\right) & \text{if } r < R \\ 0 & \text{if } r \geq R, \end{cases}$$

where

$$h = 1,$$

$$r = a \arccos[\sin\theta_c \sin\theta + \cos\theta_c \cos\theta \cos(\lambda - \lambda_c)],$$

$$R = \frac{a}{3}, \qquad \lambda_c = \frac{3\pi}{2}, \qquad \theta_c = 0, \qquad \omega = \frac{2\pi a}{12 \text{ days}}$$

and the velocity field is assumed to be constant and given by

$$\tilde{u} = +\omega(\cos\theta \cos\alpha + \sin\theta \cos\lambda \sin\alpha)$$

$$\tilde{v} = -\omega \sin\lambda \sin\alpha,$$

where α determines the axis of rotation of the flow with respect to the poles. As an example $\alpha = 0$ yields flow along the equator. The results are reported for one revolution of the initial wave that takes 12 days to complete one full revolution about the sphere. By using the mapping from spherical to Cartesian space

$$x = a \cos\theta \cos\lambda$$

$$y = a \cos\theta \sin\lambda$$

$$z = a \sin\theta, \tag{9}$$

where

$$\lambda = \arctan\left(\frac{y}{x}\right)$$

$$\theta = \arcsin\left(\frac{z}{a}\right), \tag{10}$$

we can write the initial conditions in terms of Cartesian coordinates. This results in the following velocity field:

$$u = -\tilde{u} \sin\lambda - \tilde{v} \sin\theta \cos\lambda$$

$$v = +\tilde{u} \cos\lambda - \tilde{v} \sin\theta \sin\lambda$$

$$w = +\tilde{v} \cos\theta,$$

along with the following analytic solution:

$$\varphi_{\text{exact}}(\mathbf{x}, t) = \varphi(\mathbf{x} - t\mathbf{u}, 0),$$

which is the solid body rotation of the cosine wave about the axis defined by α. Note that the mapping from spherical to Cartesian space is only done once at the beginning in order to define the problem. From then on, the problem is solved in Cartesian space. The L_2 error norm is defined as

$$\|\varphi\|_{L_2} = \left[\frac{\int_\Omega [\varphi(\mathbf{x}, t) - \varphi_{\text{exact}}(\mathbf{x}, t)]^2 \, d\Omega}{\int_\Omega [\varphi_{\text{exact}}(\mathbf{x}, t)]^2 \, d\Omega}\right]^{1/2}, \tag{11}$$

where Ω represents the element triangles, in a finite element sense. In addition to the L_2 norm, two more measures are used, namely, the first and second moments of the conservation variable, which are defined as

$$M_1 = \frac{\int_\Omega \varphi(\mathbf{x}, t) \, d\Omega}{\int_\Omega \varphi_{\text{exact}}(\mathbf{x}, t) \, d\Omega} \tag{12}$$

and

$$M_2 = \frac{\int_\Omega \varphi(\mathbf{x}, t)^2 \, d\Omega}{\int_\Omega \varphi_{\text{exact}}(\mathbf{x}, t)^2 \, d\Omega}. \tag{13}$$

These values measure the conservation properties and dissipation of the numerical method, respectively.

4. Trajectory calculations

The exact solution to (3) can be written as

$$\varphi_{\text{exact}}(\mathbf{x}, t + \Delta t) = \varphi(\mathbf{x} - \Delta t\mathbf{u}, t).$$

By applying a rotation transformation as in McDonald and Bates (1989), we get the arrival points in the rotated space

$$\lambda'_A = \arctan[\cos\theta_A \sin(\lambda_A - \lambda_\alpha), \cos\theta_A \cos(\lambda_A - \lambda_\alpha) \cos\theta_\alpha + \sin\theta_A \sin\theta_\alpha]$$

$$\theta'_A = \arcsin[\sin\theta_A \cos\theta_\alpha - \cos\theta_A \cos(\lambda_A - \lambda_\alpha) \sin\theta_\alpha],$$

which now consist of motion about the equator, only. Note that since all the points are stored in Cartesian space we must use (10) in order to get the arrival points in terms of spherical coordinates. The departure points in the rotated space are

$$\lambda'_D = \lambda'_A - \frac{\Delta t\omega}{a}$$

$$\theta'_D = \theta'_A,$$

where $\lambda_\alpha = 0$ and $\theta_\alpha = \alpha$. Using the inverse transformation, we get

$$\lambda_D = \lambda_\alpha + \arctan[\cos\theta'_D \sin\lambda'_D, \cos\theta'_D \cos\lambda'_D \cos\theta_\alpha - \sin\theta'_D \sin\theta_\alpha]$$

$$\theta_D = \arcsin[\cos\theta'_D \cos\lambda'_D \sin\theta_\alpha + \sin\theta'_D \cos\theta_\alpha], \tag{14}$$

which are the departure points in the original (unrotated) spherical space. The departure points in Cartesian space can now be obtained using the mapping (9). Equation (14) gives us the exact trajectories and so we must devise a scheme that best approximates this solution.

a. Ritchie's method

There are many ways of integrating (7) but the most common form in plane space has been the midpoint rule, namely

$$\mathbf{x}_M = \mathbf{x}_A - \frac{\Delta t}{2}\mathbf{u}\left(\mathbf{x}_M, t + \frac{\Delta t}{2}\right), \tag{15}$$

which defines a recursive scheme because $\mathbf{x}_M$ is given implicitly in the relation. In addition, this scheme also requires interpolation because $\mathbf{x}_M$ will generally not fall on a grid point. Usually, between three and five iteration loops [see Ritchie (1987)] are required to converge to the solution at which point, the departure point is calculated by

$$\mathbf{x}_D = \mathbf{x}_A - \Delta t\mathbf{u}\left(\mathbf{x}_M, t + \frac{\Delta t}{2}\right).$$

However, we have said nothing about the order of the interpolations but obviously the higher the order of the interpolant, the better the trajectory accuracy, but the greater the computer time as well. The midpoint rule yields second-order accuracy and has been used quite successfully in 2D planar space.

On the sphere, the midpoint rule has to be modified such that the new departure points computed by (15) remain on the surface of the sphere. In other words, after each iteration we must apply the projection

$$\mathbf{x}_D = \frac{a}{|\mathbf{x}_D|}\mathbf{x}_D,$$

where a is the radius of the sphere.

In fact, Ritchie's method simplifies to the midpoint rule on the surface of a sphere. In his method, we start with a Taylor series expansion about the midpoint $(t + \Delta t/2)$ up to second order to get

$$\mathbf{x}(t + \Delta t) = \mathbf{x}\left(t + \frac{\Delta t}{2}\right) + \frac{\Delta t}{2}\frac{\partial \mathbf{x}}{\partial t}\left(t + \frac{\Delta t}{2}\right) + O(\Delta t)^2.$$

Now, let $\mathbf{x}_A = \mathbf{x}(t + \Delta t)$ and $\mathbf{x}_M = \mathbf{x}(t + \Delta t/2)$ be the arrival and midpoints, respectively. After rearranging, we get

$$\mathbf{x}_M = \mathbf{x}_A - \frac{\Delta t}{2}\mathbf{u}_M,$$

which is exactly equal to (15), where $\mathbf{u}_M = \mathbf{u}(\mathbf{x}_M, t + \Delta t/2)$. However, we need to add a correction factor b in order to constrain the new iterated point to remain on the sphere. Thus, we require

$$\mathbf{x}_M = b\left(\mathbf{x}_A - \frac{\Delta t}{2}\mathbf{u}_M\right) \tag{16}$$

such that

$$|\mathbf{x}_M| = a.$$

Taking the magnitude of (16) and rearranging we get

$$b = \frac{a}{\left[a^2 - \Delta t\mathbf{x}_A \cdot \mathbf{u}_M + \left(\frac{\Delta t}{2}\right)^2 \mathbf{u}_M \cdot \mathbf{u}_M\right]^{1/2}},$$

which is similar to the result in Ritchie (1987) but for a two-time-level scheme. From Ritchie (1987), we get the departure points from the relation

$$\mathbf{x}_D = \frac{2\mathbf{x}_M \cdot \mathbf{x}_A}{a^2}\mathbf{x}_M - \mathbf{x}_A,$$

which can be simplified by using the definition of a dot product

$$\mathbf{x}_M \cdot \mathbf{x}_A = |\mathbf{x}_M||\mathbf{x}_A| \cos\theta$$

to

$$\mathbf{x}_M = \frac{\mathbf{x}_D + \mathbf{x}_A}{2\cos\theta}.$$

If we take the midpoint to be the average between the arrival and departure points and then project it on to the sphere, we arrive at the relation

$$\mathbf{x}_M = b\left(\frac{\mathbf{x}_D + \mathbf{x}_A}{2}\right).$$

By once again enforcing that the point remains on the sphere, we get

$$b = \left[\frac{2}{1 + \cos 2\theta}\right]^{1/2}$$

and by using the trigonometric identity $\cos 2\theta = 2\cos^2\theta - 1$ we now get

$$b = \frac{1}{\cos\theta},$$

which recovers Ritchie's result. Thus, Ritchie's method is exactly the midpoint integration rule with a modification that projects the iterated point onto the surface of the sphere.

b. McGregor's method

Another possibility for integrating (7) is the noniterative scheme of McGregor. From McGregor (1993), we write a Taylor series expansion for the departure point $\mathbf{x}(t)$ about the arrival point $\mathbf{x}(t + \Delta t)$ along the characteristics as

$$\mathbf{x}(t) = \mathbf{x}(t + \Delta t) + \sum_{n=1}^{N} \frac{(-\Delta t)^n}{n!}\frac{d^n\mathbf{x}}{dt^n}(t + \Delta t) + O(\Delta t, \Delta x)^{N+1},$$

where

$$\frac{d}{dt} = \frac{\partial}{\partial t} + \mathbf{u} \cdot \nabla \approx \hat{\mathbf{u}} \cdot \nabla$$

and

$$\hat{\mathbf{u}} = \mathbf{u}\left(\mathbf{x}(t + \Delta t),\, t + \frac{\Delta t}{2}\right)$$

[see McGregor (1993)]. Therefore, the only thing left to do is to obtain the derivatives in the gradient operator ∇. If we are using rectangular grids then we can write the derivatives in the standard centered finite difference form

$$\frac{\partial \varphi}{\partial x}(x, y, z) = \frac{\varphi(x + \Delta x, y, z) - \varphi(x - \Delta x, y, z)}{2\Delta x}$$

$$\frac{\partial \varphi}{\partial y}(x, y, z) = \frac{\varphi(x, y + \Delta y, z) - \varphi(x, y - \Delta y, z)}{2\Delta y}$$

$$\frac{\partial \varphi}{\partial z}(x, y, z) = \frac{\varphi(x, y, z + \Delta z) - \varphi(x, y, z - \Delta z)}{2\Delta z},$$

yielding a second-order accurate derivative in space. Higher derivatives are also readily available reapplying this relation. But what if the grid is unstructured? In this case, we must compute the derivatives in a finite element sense. But first, let us introduce the linear triangular finite element basis functions on the sphere.

5. Basis functions

Linear natural coordinates on a triangle in 3D Cartesian space can be written as

$$\psi_i(x, y, z) = \frac{a_i x + b_i y + c_i z}{\text{deter } \Delta}, \tag{17}$$

where

$$a_i = y_j z_k - y_k z_j, \qquad b_i = x_k z_j - x_j z_k,$$

$$c_i = x_j y_k - x_k y_j,$$

and

$$\text{deter } \Delta = \begin{vmatrix} x_1 & x_2 & x_3 \\ y_1 & y_2 & y_3 \\ z_1 & z_2 & z_3 \end{vmatrix},$$

where i, j, k are cyclical, that is, if $i = 1$, then $j = 2$, and $k = 3$, and so on. By using the definition of the natural coordinates (17) and the fact that the three nodes on each triangle define a plane

$$\mathbf{N} \cdot (\mathbf{x} - \mathbf{x}_1) = 0,$$

where $\mathbf{N}$ is the outward pointing normal to the triangle and defined by

$$\mathbf{N} = (\mathbf{x}_2 - \mathbf{x}_1) \times (\mathbf{x}_3 - \mathbf{x}_1) = \begin{vmatrix} \hat{\mathbf{i}} & \hat{\mathbf{j}} & \hat{\mathbf{k}} \\ x_2 - x_1 & y_2 - y_1 & z_2 - z_1 \\ x_3 - x_1 & y_3 - y_1 & z_3 - z_1 \end{vmatrix}, \tag{18}$$

it can be shown that the natural coordinates satisfy the condition

$$\psi_1(x, y, z) + \psi_2(x, y, z) + \psi_3(x, y, z) = 1$$

(see the appendix for the proofs and derivations concerning these basis functions). This is a necessary condition for a consistent and monotonic interpolation. These natural coordinates can now be used as the finite element basis functions. Integration by parts reveals that any integral of the following form involving these basis functions can be obtained in closed form by the relation

$$\int \psi_1^\alpha \psi_2^\beta \psi_3^\gamma \, d\Omega = \frac{\text{deter } \Delta \alpha! \beta! \gamma!}{(\alpha + \beta + \gamma + 2)!}. \tag{19}$$

This relation is almost identical to the closed form solution for linear triangles on the plane given by Silvester (1969). For the special case that the three-dimensional domain lies entirely on a plane, both integration rules are equivalent. Using these basis functions, we can now construct the derivatives at the grid points in a finite element sense.

Derivatives

We can construct the derivatives in the following manner: let

$$\varphi^e(x, y, z) = \sum_{j=1}^{3} \psi_j(x, y, z) \varphi_j \tag{20}$$

denote the value of φ^e within the element, ψ_j the basis functions, and φ_j the value of the conservation variable at the vertices (grid points) of the element in question. From (20) we get the derivatives within the element to be

$$\frac{\partial \varphi^e}{\partial x}(x, y, z) = \sum_{j=1}^{3} \frac{\partial \psi_j}{\partial x}(x, y, z) \varphi_j$$

$$\frac{\partial \varphi^e}{\partial y}(x, y, z) = \sum_{j=1}^{3} \frac{\partial \psi_j}{\partial y}(x, y, z) \varphi_j$$

$$\frac{\partial \varphi^e}{\partial z}(x, y, z) = \sum_{j=1}^{3} \frac{\partial \psi_j}{\partial z}(x, y, z) \varphi_j, \tag{21}$$

where

$$\frac{\partial \psi_j}{\partial x}(x, y, z) = \frac{a_j}{\text{deter } \Delta}$$

$$\frac{\partial \psi_j}{\partial y}(x, y, z) = \frac{b_j}{\text{deter } \Delta}$$

$$\frac{\partial \psi_j}{\partial z}(x, y, z) = \frac{c_j}{\text{deter } \Delta},$$

from (17).

However, we need the derivatives on the grid points and not within the elements. If we knew these derivatives, then we could write them as

$$\frac{\partial \varphi^e}{\partial x}(x, y, z) = \sum_{j=1}^{3} \psi_j(x, y, z)\frac{\partial \varphi_j}{\partial x}$$

$$\frac{\partial \varphi^e}{\partial y}(x, y, z) = \sum_{j=1}^{3} \psi_j(x, y, z)\frac{\partial \varphi_j}{\partial y}$$

$$\frac{\partial \varphi^e}{\partial z}(x, y, z) = \sum_{j=1}^{3} \psi_j(x, y, z)\frac{\partial \psi_j}{\partial z}. \tag{22}$$

Equating these relations with (21) and employing the finite element method, we can construct a set of integral equations, namely

$$\int_\Omega \psi_i\psi_j \, d\Omega \frac{\partial \varphi_j}{\partial x} = \int_\Omega \psi_i \frac{\partial \psi_j}{\partial x} \, d\Omega \varphi_j$$

$$\int_\Omega \psi_i\psi_j \, d\Omega \frac{\partial \varphi_j}{\partial y} = \int_\Omega \psi_i \frac{\partial \psi_j}{\partial y} \, d\Omega \varphi_j$$

$$\int_\Omega \psi_i\psi_j \, d\Omega \frac{\partial \varphi_j}{\partial z} = \int_\Omega \psi_i \frac{\partial \psi_j}{\partial z} \, d\Omega \varphi_j, \tag{23}$$

for $i, j = 1, \ldots, 3$ which is symmetric and, depending on the node number ordering, tightly banded. Using Eqs. (17) and (19), Eq. (23) results in the following elemental matrix equations:

$$\frac{\text{deter } \Delta}{24}\begin{bmatrix} 2 & 1 & 1 \\ 1 & 2 & 1 \\ 1 & 1 & 2 \end{bmatrix}\begin{Bmatrix} \dfrac{\partial \varphi_1}{\partial x} \\ \dfrac{\partial \varphi_2}{\partial x} \\ \dfrac{\partial \varphi_3}{\partial x} \end{Bmatrix}$$

$$= \frac{\text{deter } \Delta}{24 \text{ deter } \Delta}\begin{Bmatrix} a_1\varphi_1 + a_2\varphi_2 + a_3\varphi_3 \\ a_1\varphi_1 + a_2\varphi_2 + a_3\varphi_3 \\ a_1\varphi_1 + a_2\varphi_2 + a_3\varphi_3 \end{Bmatrix}, \tag{24}$$

with similar relations for the y and z terms. The global system composed of these elemental matrix equations requires the inversion of a sparse but tightly banded matrix. This potential bottleneck can be bypassed by diagonalizing the elemental equations yielding

$$\begin{bmatrix} 1 & 0 & 0 \\ 0 & 1 & 0 \\ 0 & 0 & 1 \end{bmatrix}\begin{Bmatrix} \dfrac{\partial \varphi_1}{\partial x} \\ \dfrac{\partial \varphi_2}{\partial x} \\ \dfrac{\partial \varphi_3}{\partial x} \end{Bmatrix} = \frac{1}{4 \text{ deter } \Delta}\begin{Bmatrix} a_1\varphi_1 + a_2\varphi_2 + a_3\varphi_3 \\ a_1\varphi_1 + a_2\varphi_2 + a_3\varphi_3 \\ a_1\varphi_1 + a_2\varphi_2 + a_3\varphi_3 \end{Bmatrix},$$

which can be solved explicitly for the derivatives. The second derivatives within the element can now be written as

$$\frac{\partial^2 \varphi^e}{\partial x^2}(x, y, z) = \sum_{j=1}^{3} \psi_j(x, y, z)\frac{\partial^2 \varphi_j}{\partial x^2}$$

$$\frac{\partial^2 \varphi^e}{\partial y^2}(x, y, z) = \sum_{j=1}^{3} \psi_j(x, y, z)\frac{\partial^2 \varphi_j}{\partial y^2}$$

$$\frac{\partial^2 \varphi^e}{\partial z^2}(x, y, z) = \sum_{j=1}^{3} \psi_j(x, y, z)\frac{\partial^2 \varphi_j}{\partial z^2},$$

that is, assuming we knew the second derivatives at the grid points. Taking the derivatives of (22) we get

$$\frac{\partial^2 \varphi^e}{\partial x^2}(x, y, z) = \sum_{j=1}^{3} \frac{\partial \psi_j}{\partial x}(x, y, z)\frac{\partial \varphi_j}{\partial x}$$

$$\frac{\partial^2 \varphi^e}{\partial y^2}(x, y, z) = \sum_{j=1}^{3} \frac{\partial \psi_j}{\partial y}(x, y, z)\frac{\partial \varphi_j}{\partial y}$$

$$\frac{\partial^2 \varphi^e}{\partial z^2}(x, y, z) = \sum_{j=1}^{3} \frac{\partial \psi_j}{\partial z}(x, y, z)\frac{\partial \varphi_j}{\partial z},$$

where the derivatives of φ_j are the first derivatives at the grid points obtained from (24). Equating these two sets of relations and once again employing the finite element method, we obtain the equations

$$\int_\Omega \psi_i\psi_j \, d\Omega \frac{\partial^2 \varphi_j}{\partial x^2} = \int_\Omega \psi_i \frac{\partial \psi_j}{\partial x} \, d\Omega \frac{\partial \varphi_j}{\partial x}$$

$$\int_\Omega \psi_i\psi_j \, d\Omega \frac{\partial^2 \varphi_j}{\partial y^2} = \int_\Omega \psi_i \frac{\partial \psi_j}{\partial y} \, d\Omega \frac{\partial \varphi_j}{\partial y}$$

$$\int_\Omega \psi_i\psi_j \, d\Omega \frac{\partial^2 \varphi_j}{\partial z^2} = \int_\Omega \psi_i \frac{\partial \psi_j}{\partial z} \, d\Omega \frac{\partial \varphi_j}{\partial z}, \tag{25}$$

which simplify to the following element matrix relations

$$\frac{\text{deter } \Delta}{24}\begin{bmatrix} 2 & 1 & 1 \\ 1 & 2 & 1 \\ 1 & 1 & 2 \end{bmatrix}\begin{Bmatrix} \dfrac{\partial^2 \varphi_1}{\partial x^2} \\ \dfrac{\partial^2 \varphi_2}{\partial x^2} \\ \dfrac{\partial^2 \varphi_3}{\partial x^2} \end{Bmatrix}$$

$$= \frac{\text{deter } \Delta}{24 \text{ deter } \Delta}\begin{Bmatrix} a_1\dfrac{\partial \varphi_1}{\partial x} + a_2\dfrac{\partial \varphi_2}{\partial x} + a_3\dfrac{\partial \varphi_3}{\partial x} \\ a_1\dfrac{\partial \varphi_1}{\partial x} + a_2\dfrac{\partial \varphi_2}{\partial x} + a_3\dfrac{\partial \varphi_3}{\partial x} \\ a_1\dfrac{\partial \varphi_1}{\partial x} + a_2\dfrac{\partial \varphi_2}{\partial x} + a_3\dfrac{\partial \varphi_3}{\partial x} \end{Bmatrix}, \tag{26}$$

where once again, the relations for the y and z terms are immediately obvious. The diagonalized version yields

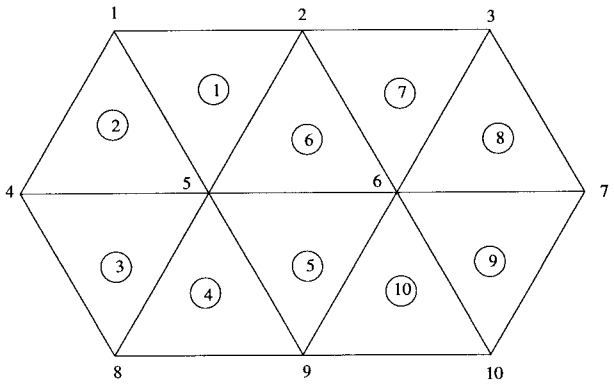

FIG. 1. The element-wise contribution of the surrounding elements to the grid points.

$$\begin{bmatrix} 1 & 0 & 0 \\ 0 & 1 & 0 \\ 0 & 0 & 1 \end{bmatrix} \begin{Bmatrix} \dfrac{\partial^2 \varphi_1}{\partial x^2} \\ \dfrac{\partial^2 \varphi_2}{\partial x^2} \\ \dfrac{\partial^2 \varphi_3}{\partial x^2} \end{Bmatrix} = \frac{1}{4 \text{ deter } \Delta} \begin{Bmatrix} a_1 \dfrac{\partial \varphi_1}{\partial x} + a_2 \dfrac{\partial \varphi_2}{\partial x} + a_3 \dfrac{\partial \varphi_3}{\partial x} \\ a_1 \dfrac{\partial \varphi_1}{\partial x} + a_2 \dfrac{\partial \varphi_2}{\partial x} + a_3 \dfrac{\partial \varphi_3}{\partial x} \\ a_1 \dfrac{\partial \varphi_1}{\partial x} + a_2 \dfrac{\partial \varphi_2}{\partial x} + a_3 \dfrac{\partial \varphi_3}{\partial x} \end{Bmatrix},$$

which, again, does not require the inversion of a large global matrix. Higher-order derivatives can be obtained by continuing this process. Note that Eqs. (24) and (26) may appear to imply that $\partial\varphi_1/\partial x = \partial\varphi_2/\partial x = \partial\varphi_3/\partial x$ and similarly for all derivatives. However, these are elemental equations and the global equations are obtained by summing the contribution of all the triangular elements surrounding each node point. Because the basis functions are linear, then the derivatives within the element will be constants so that Eqs. (24) and (26) say that the contribution of each triangular element to its three vertices is a constant value. In Fig. 1 we can see that grid point 5 will get contributions from elements 1–6, while grid point 6 will get contributions from elements 5–10. As a result, all of the gridpoint derivatives will have unique values.

6. Derivative accuracy

Before we study the accuracy of the trajectory calculations using the results from the previous two sections it is wise to first know the accuracy of the derivatives themselves. Let us apply the 3D linear basis functions on a plane. We perform these numerical experiments on the plane using a structured grid in order to compare our finite element derivatives with the standard centered finite differences. On this plane, let $z = c$ where c is some constant. Therefore our basis functions simplify as follows:

$$\psi_i = \frac{a_i x + b_i y + c_i}{\text{deter } \Delta},$$

where

TABLE 1. Derivative accuracy using centered finite differences for the cosine function in planar space on the crisscross grid.

Grid points	$\left\|\frac{\partial f}{\partial x}\right\|_{L_2}$	$\left\|\frac{\partial f}{\partial y}\right\|_{L_2}$	$\left\|\frac{\partial^2 f}{\partial x^2}\right\|_{L_2}$	$\left\|\frac{\partial^2 f}{\partial y^2}\right\|_{L_2}$	$\left\|\frac{\partial^2 f}{\partial x \partial y}\right\|_{L_2}$
11 × 11	0.2498	0.2498	0.5076	0.5076	0.5174
21 × 21	0.1127	0.1127	0.3655	0.3655	0.3288
41 × 41	0.0346	0.0346	0.2146	0.2146	0.2113
61 × 61	0.0174	0.0174	0.1602	0.1602	0.1667
81 × 81	0.0108	0.0108	0.1325	0.1325	0.1430

$$a_i = y_j - y_k, \qquad b_i = x_k - x_j, \qquad c_i = x_j y_k - x_k y_j,$$

and

$$\text{deter } \Delta = \begin{vmatrix} x_1 & x_2 & x_3 \\ y_1 & y_2 & y_3 \\ 1 & 1 & 1 \end{vmatrix},$$

where $z = c$ has been factored out from all of the relations. Recall that these functions have the exact integration rules obtained by

$$\int \psi_1^\alpha \psi_2^\beta \psi_3^\gamma \, d\Omega = \frac{\text{deter } \Delta \alpha! \beta! \gamma!}{(\alpha + \beta + \gamma + 2)!},$$

which now yields the usual linear triangular finite element basis functions on the plane as in Silvester (1969). To test the accuracy of the numerical derivatives, we shall use the cosine function

$$f(\mathbf{x}) = \begin{cases} \dfrac{h}{2}\left(1 + \cos\dfrac{\pi r}{R}\right) & \text{if } r < R \\ 0 & \text{if } r \geq R \end{cases}$$

with

$$r = \sqrt{(x - x_c)^2 + (y - y_c)^2}, \qquad (x_c, y_c) = (0, 0),$$

$$[x, y] \in [-1, +1], \qquad R = \frac{1}{2}.$$

By defining a normalized L_2 norm such as

$$\left\|\frac{\partial f}{\partial x}\right\|_{L_2} = \left[\frac{\displaystyle\int_\Omega \left[\frac{\partial f}{\partial x}(\mathbf{x}) - \frac{\partial f}{\partial x_{\text{exact}}}(\mathbf{x})\right]^2 d\Omega}{\displaystyle\int_\Omega \left[\frac{\partial f}{\partial x_{\text{exact}}}(\mathbf{x})\right]^2 d\Omega}\right]^{1/2},$$

for all of the derivatives, we can now measure the accuracy of our numerical derivatives. Tables 1, 2, and 3 list the first and second derivative results for various grid sizes using centered finite differences, finite elements with a full matrix, and finite elements with a diagonalized matrix, respectively. An example of the structure of the grids used is illustrated in Fig. 2 for the 11 × 11 point case. The tabulated results show that the finite element derivatives are superior to the finite differences but this approach requires the inversion of a

TABLE 2. Derivative accuracy using finite elements with a full matrix for the cosine function in planar space on the crisscross grid.

Grid points	$\left\|\frac{\partial f}{\partial x}\right\|_{L_2}$	$\left\|\frac{\partial f}{\partial y}\right\|_{L_2}$	$\left\|\frac{\partial^2 f}{\partial x^2}\right\|_{L_2}$	$\left\|\frac{\partial^2 f}{\partial y^2}\right\|_{L_2}$	$\left\|\frac{\partial^2 f}{\partial x \partial y}\right\|_{L_2}$
11 × 11	0.1536	0.1536	0.5678	0.5678	0.3170
21 × 21	0.1047	0.1047	0.3806	0.3806	0.2959
41 × 41	0.0262	0.0262	0.2251	0.2251	0.1886
61 × 61	0.0162	0.0162	0.1712	0.1712	0.1508
81 × 81	0.0087	0.0087	0.1422	0.1422	0.1263

matrix. For this reason, we have also included the diagonalized version, which does not require this inversion. The results show that the diagonalized version is inferior to the full matrix version but if we are concerned with efficiency, then this faster version is more appropriate. Let us now look at the formal order of accuracy analysis of the finite element type numerical derivatives.

Order of accuracy analysis

The structured crisscross grid illustrated in Fig. 2 was selected for our study because it has the least amount of biasing. This is important because the spherical geodesic grid has little or no biasing on the sphere. The crisscross grid has two types of gridpoint contributions from the surrounding elements that are illustrated in Figs. 3 and 4. The first type of contribution (illustrated in Fig. 3) has derivatives given by

$$\frac{\partial f_{i,j}}{\partial x} = \frac{(f_{i+1,j} - f_{i-1,j})}{2\Delta x} + O(\Delta x^2)$$

$$\frac{\partial^2 f_{i,j}}{\partial x^2} = \frac{(f_{i+2,j} - 2f_{i,j} + f_{i-2,j})}{4\Delta x^2} + O(\Delta x^2)$$

$$\frac{\partial^2 f_{i,j}}{\partial x \partial y} = \frac{(f_{i+1,j+1} - f_{i-1,j+1} - f_{i+1,j-1} + f_{i-1,j-1})}{4\Delta x \Delta y} + O(\Delta x^2, \Delta y^2),$$

where the derivatives in y are immediately obvious. The orders O given in these relations denote the order of accuracy of the derivatives. These derivatives are all second-order accurate in both x and y. In fact, they yield the exact same derivative formulas obtained with centered finite differencing. The second type of contribution (Fig. 4) has the derivatives

$$\frac{\partial f_{i,j}}{\partial x} = \frac{(f_{i+1,j+1} - f_{i-1,j+1})}{8\Delta x} + \frac{2(f_{i+1,j} - f_{i-1,j})}{8\Delta x} + \frac{(f_{i+1,j-1} - f_{i-1,j-1})}{8\Delta x} + O(\Delta x^2, \Delta y^2),$$

TABLE 3. Derivative accuracy using finite elements with a diagonalized matrix for the cosine function in planar space on the crisscross grid.

Grid points	$\left\|\frac{\partial f}{\partial x}\right\|_{L_2}$	$\left\|\frac{\partial f}{\partial y}\right\|_{L_2}$	$\left\|\frac{\partial^2 f}{\partial x^2}\right\|_{L_2}$	$\left\|\frac{\partial^2 f}{\partial y^2}\right\|_{L_2}$	$\left\|\frac{\partial^2 f}{\partial x \partial y}\right\|_{L_2}$
11 × 11	0.2879	0.2879	0.7452	0.7452	0.6645
21 × 21	0.1341	0.1341	0.4519	0.4519	0.3874
41 × 41	0.0382	0.0382	0.2718	0.2718	0.2402
61 × 61	0.0207	0.0207	0.2095	0.2095	0.1884
81 × 81	0.0121	0.0121	0.1764	0.1764	0.1618

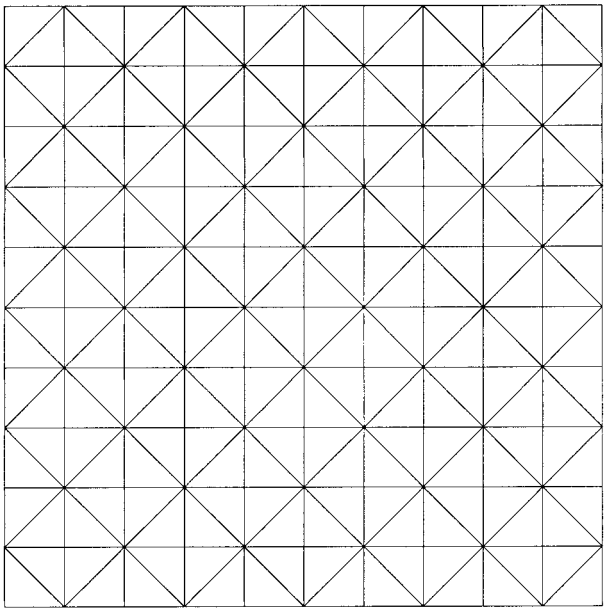

FIG. 2. The 11 × 11 point crisscross grid used for the derivative analysis.

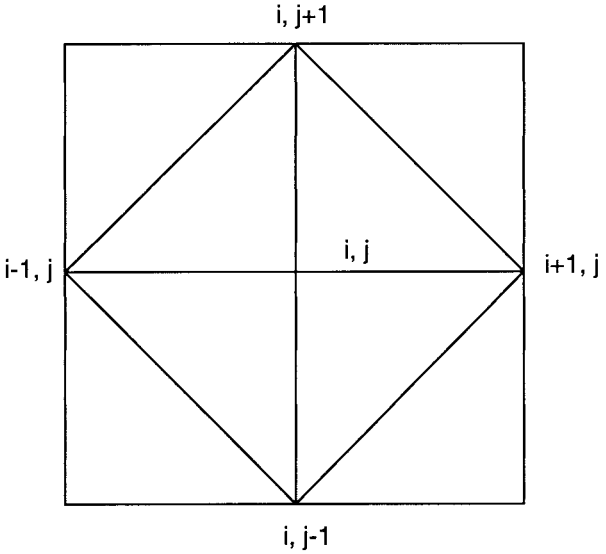

FIG. 3. The first type of element contribution to the grid points of the crisscross grid.

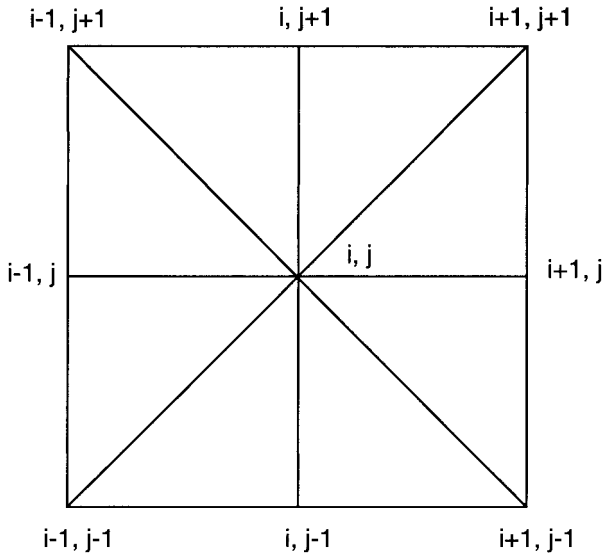

FIG. 4. The second type of element contribution to the grid points of the crisscross grid.

$$\frac{\partial^2 f_{i,j}}{\partial x^2} = \frac{(f_{i+2,j+2} - 2f_{i,j+2} + f_{i-2,j+2})}{64\Delta x^2} + \frac{4(f_{i+2,j+1} - 2f_{i,j+1} + f_{i-2,j+1})}{64\Delta x^2} + \frac{6(f_{i+2,j} - 2f_{i,j} + f_{i-2,j})}{64\Delta x^2} + \frac{4(f_{i+2,j-1} - 2f_{i,j-1} + f_{i-2,j-1})}{64\Delta x^2} + \frac{(f_{i+2,j-2} - 2f_{i,j-2} + f_{i-2,j-2})}{64\Delta x^2} + O(\Delta x^2, \Delta y^2),$$

and

$$\frac{\partial^2 f_{i,j}}{\partial x \partial y} = \frac{(f_{i+2,j+2} - f_{i+2,j-2} - f_{i-2,j+2} + f_{i-2,j-2})}{64\Delta x \Delta y} + \frac{2(f_{i+2,j+1} - f_{i+2,j-1} - f_{i-2,j+1} + f_{i-2,j-1})}{64\Delta x \Delta y} + \frac{2(f_{i+1,j+2} - f_{i+1,j-2} - f_{i-1,j+2} + f_{i-1,j-2})}{64\Delta x \Delta y} + \frac{4(f_{i+1,j+1} - f_{i+1,j-1} - f_{i-1,j+1} + f_{i-1,j-1})}{64\Delta x \Delta y} + O(\Delta x^2, \Delta y^2),$$

which are all second order. Thus even with the diagonalized version of the derivatives, we are guaranteed an order of accuracy similar to centered finite differences, regardless of the structure of the grid. This order of accuracy analysis is given only to compare the finite element derivatives to the finite difference derivatives.

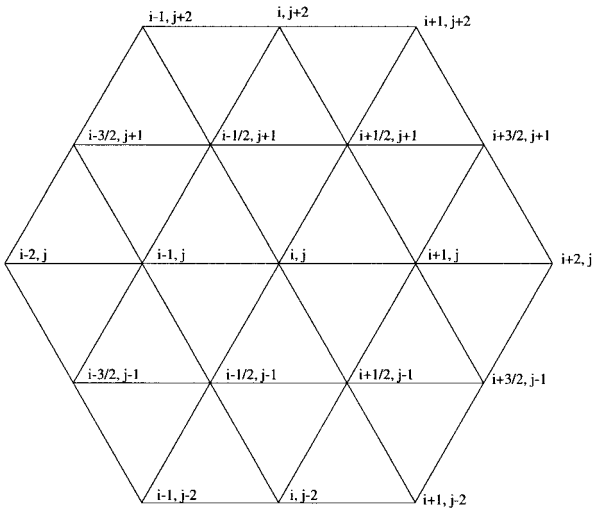

FIG. 5. The differencing stencil for the finite element derivatives on the spherical geodesic grid.

However, the real interest is in determining the finite element derivatives on the hexagonal-type stencils that arise in the spherical geodesic grids and is illustrated in Fig. 5. In this case, we arrive at the following derivatives:

$$\frac{\partial f_{i,j}}{\partial x} = \frac{(f_{i+(1/2),j+1} - f_{i-(1/2),j+1})}{6\Delta x} + \frac{2(f_{i+1,j} - f_{i-1,j})}{6\Delta x} + \frac{(f_{i+(1/2),j-1} - f_{i-(1/2),j-1})}{6\Delta x} + O(\Delta x^2, \Delta y^2),$$

$$\frac{\partial f_{i,j}}{\partial y} = \frac{(f_{i+(1/2),j+1} - f_{i+(1/2),j-1})}{4\Delta y} + \frac{(f_{i-(1/2),j+1} - f_{i-(1/2),j-1})}{4\Delta y} + O(\Delta x^2, \Delta y^2),$$

$$\frac{\partial^2 f_{i,j}}{\partial x^2} = \frac{(f_{i+1,j+2} - 2f_{i,j+2} + f_{i-1,j+2})}{36\Delta x^2} + \frac{4(f_{i+(3/2),j+1} - f_{i+(1/2),j+1} - f_{i-(1/2),j+1} + f_{i-(3/2),j+1})}{36\Delta x^2} + \frac{2(2f_{i+2,j} + f_{i+1,j} - 6f_{i,j} + f_{i-1,j} + 2f_{i-2,j})}{36\Delta x^2} + \frac{4(f_{i+(3/2),j-1} - f_{i+(1/2),j-1} - f_{i-(1/2),j-1} + f_{i-(3/2),j-1})}{36\Delta x^2} + \frac{(f_{i+1,j-2} - 2f_{i,j-2} + f_{i-1,j-2})}{36\Delta x^2} + O(\Delta x^2, \Delta y^2),$$

$$\frac{\partial^2 f_{i,j}}{\partial y^2} = \frac{(f_{i+1,j+2} - 2f_{i+1,j} + f_{i+1,j-2})}{16\Delta y^2} + \frac{2(f_{i,j+2} - 2f_{i,j} + f_{i,j-2})}{16\Delta y^2} + \frac{(f_{i-1,j+2} - 2f_{i-1,j} + f_{i-1,j-2})}{16\Delta y^2} + O(\Delta x^2, \Delta y^2),$$

TABLE 4. Trajectory accuracy for the exact trajectories, midpoint rule, and McGregor's noninterpolating scheme for values of $N = 1, \ldots, 4$ with $\sigma = 1.13$ on the spherical geodesic grid with 642 points after one revolution for $\alpha = 0$.

Trajectory method	$\|\mathbf{x}_D\|_{L_2}$	$\|\varphi\|_{L_2}$	M_1	M_2
Exact	0.0000	0.0917	1.0071	0.9783
Midpoint rule	0.0026	0.1132	1.0069	9.9809
$N = 1$	0.0358	0.4743	1.0127	0.6064
$N = 2$	0.0041	0.1724	1.0064	0.9764
$N = 3$	0.0003	0.0918	1.0069	0.9854
$N = 4$	0.0002	0.0917	1.0069	0.9844

TABLE 5. Trajectory accuracy for the exact trajectories, midpoint rule, and McGregor's noninterpolating scheme for values of $N = 1, \ldots, 4$ with $\sigma = 2.27$ on the spherical geodesic grid with 2562 points after one revolution for $\alpha = 0$.

Trajectory method	$\|\mathbf{x}_D\|_{L_2}$	$\|\varphi\|_{L_2}$	M_1	M_2
Exact	0.0000	0.0195	0.9988	0.9996
Midpoint rule	0.0008	0.0386	0.9988	0.9995
$N = 1$	0.0358	0.4684	1.0050	0.6271
$N = 2$	0.0041	0.1506	0.9980	1.0001
$N = 3$	0.0003	0.0210	0.9987	1.0057
$N = 4$	0.0002	0.0206	0.9987	1.0057

and

$$\frac{\partial^2 f_{i,j}}{\partial x \partial y} = \frac{(f_{i+1,j+2} - f_{i+1,j-2} - f_{i-1,j+2} + f_{i-1,j-2})}{24\Delta x \Delta y} + \frac{2(f_{i+(3/2),j+1} - f_{i+(3/2),j-1} - f_{i-(3/2),j+1} + f_{i-(3/2),j-1})}{24\Delta x \Delta y} + \frac{2(f_{i+(1/2),j+1} - f_{i+(1/2),j-1} - f_{i-(1/2),j+1} + f_{i-(1/2),j-1})}{24\Delta x \Delta y} + O(\Delta x^2, \Delta y^2),$$

which are also second-order accurate.

7. Trajectory accuracy

In a similar manner described in McGregor (1993), we define the accuracy of the trajectories by the normalized L_2 norm

$$\|\mathbf{x}_D\|_{L_2} = \left[\frac{\int_\Omega [\mathbf{x}_D - \mathbf{x}_D^{\text{exact}}]^2 \, d\Omega}{\int_\Omega [\mathbf{x}_D - \mathbf{x}_A]^2 \, d\Omega} \right]^{1/2}. \quad (27)$$

The results for various methods of obtaining the trajectories are illustrated in Tables 4 and 5 where the spherical geodesic grid contains 642 points with a Courant number $\sigma = 1.13$, and 2562 points with $\sigma = 2.27$, respectively. These results are all shown for $\alpha = 0$ meaning that the wave moves along the equator. A schematic of the grid containing 2562 grid points is illustrated in Fig. 6. The results point toward the same conclusions, namely, that McGregor's scheme is extremely good and that it increases in accuracy as the number of terms in the Taylor series N is increased. However, very little is gained beyond values of 4, which is in agreement with the findings in McGregor (1993). For this reason, results for $N > 4$ are not shown.

8. Conclusions

The determination of departure points are explored for spherical geodesic grids in Cartesian space. The midpoint rule, which is an interpolating and iterative scheme, is compared against McGregor's noninterpolating and noniterative method. McGregor's method yields better results but no benefits are gained by using more than four terms in the Lagrangian Taylor series expansion. McGregor (1993) showed how to apply this scheme on rectangular grids. This paper extends McGregor's method to unstructured triangular grids. The difficulty in applying McGregor's method to unstructured grids is that derivatives at the grid points need to be obtained in order to get the higher-order Taylor series expansion terms. This can be done for unstructured grids by constructing the derivatives in an element by element approach. This approach is illustrated for the unstructured triangular grids composing the spherical geodesic grids by using the linear triangular basis functions introduced in Giraldo (1997). Once these functions have been defined, we can then apply the strategy for forming derivatives illustrated here. The numerical derivatives are compared against analytic solutions for the cosine hill function and its derivatives.

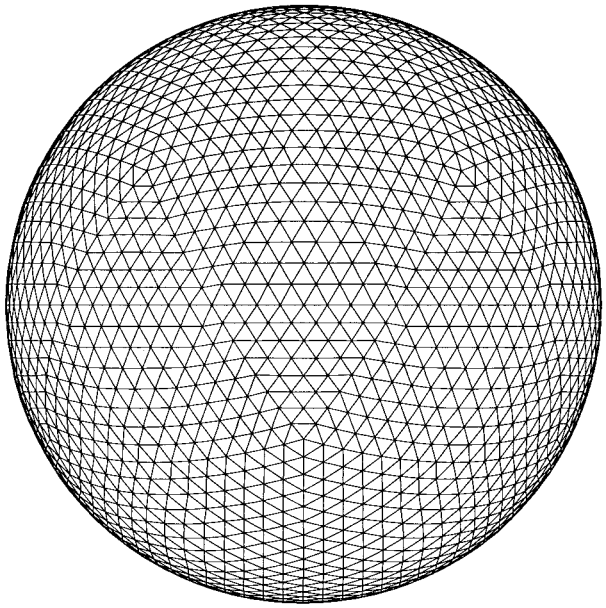

FIG. 6. The spherical geodesic grid with 2562 points.

These results show that the numerical derivatives are quite accurate especially for the low-order derivatives. An order of accuracy analysis is performed that demonstrates the order of accuracy of this strategy to be second order. Therefore, it is quite similar to the centered finite difference approach used in McGregor (1993), but for unstructured triangular grids.

Acknowledgments. I would like to thank the Office of Naval Research for supporting this work through Program PE-0602435N.

APPENDIX

3D Triangular Basis Function

Theorem 1. The basis functions

$$\psi_i(\mathbf{x}) = \frac{a_i x + b_i y + c_i z}{\text{deter } \Delta}, \tag{A1}$$

where

$$a_i = y_j z_k - y_k z_j, \qquad b_i = x_k z_j - x_j z_k, \qquad c_i = x_j y_k - x_k y_j,$$

and

$$\text{deter } \Delta = \begin{vmatrix} x_1 & x_2 & x_3 \\ y_1 & y_2 & y_3 \\ z_1 & z_2 & z_3 \end{vmatrix},$$

define a set of linear cardinal basis functions, that is,

$$\psi_i(\mathbf{x}_j) = \begin{cases} 1 & \text{if } i = j \\ 0 & \text{if } i \neq j. \end{cases}$$

Proof. The conditions to be satisfied by a linear interpolation on a triangle in three-dimensional space are the following:

$$\begin{aligned} x &= \psi_1(\mathbf{x})x_1 + \psi_2(\mathbf{x})x_2 + \psi_3(\mathbf{x})x_3 \\ y &= \psi_1(\mathbf{x})y_1 + \psi_2(\mathbf{x})y_2 + \psi_3(\mathbf{x})y_3 \\ z &= \psi_1(\mathbf{x})z_1 + \psi_2(\mathbf{x})z_2 + \psi_3(\mathbf{x})z_3, \end{aligned} \tag{A2}$$

which just says that the coordinates within the triangular element are dependent on the vertices of that element. Equation (A2) can be written in the following matrix form:

$$\begin{bmatrix} x_1 & x_2 & x_3 \\ y_1 & y_2 & y_3 \\ z_1 & z_2 & z_3 \end{bmatrix} \begin{bmatrix} \psi_1(\mathbf{x}) \\ \psi_2(\mathbf{x}) \\ \psi_3(\mathbf{x}) \end{bmatrix} = \begin{bmatrix} x \\ y \\ z \end{bmatrix}.$$

Using Cramer's rule to invert this matrix system yields the following relations for the natural coordinates,

$$\psi_1(\mathbf{x}) = \frac{\begin{vmatrix} x & x_2 & x_3 \\ y & y_2 & y_3 \\ z & z_2 & z_3 \end{vmatrix}}{\begin{vmatrix} x_1 & x_2 & x_3 \\ y_1 & y_2 & y_3 \\ z_1 & z_2 & z_3 \end{vmatrix}}, \qquad \psi_2(\mathbf{x}) = \frac{\begin{vmatrix} x_1 & x & x_3 \\ y_1 & y & y_3 \\ z_1 & z & z_3 \end{vmatrix}}{\begin{vmatrix} x_1 & x_2 & x_3 \\ y_1 & y_2 & y_3 \\ z_1 & z_2 & z_3 \end{vmatrix}},$$

$$\psi_3(\mathbf{x}) = \frac{\begin{vmatrix} x_1 & x_2 & x \\ y_1 & y_2 & y \\ z_1 & z_2 & z \end{vmatrix}}{\begin{vmatrix} x_1 & x_2 & x_3 \\ y_1 & y_2 & y_3 \\ z_1 & z_2 & z_3 \end{vmatrix}},$$

which can be written more compactly in terms of scalar and vector products as

$$\psi_1(\mathbf{x}) = \frac{\mathbf{x} \cdot (\mathbf{x}_2 \times \mathbf{x}_3)}{\mathbf{x}_1 \cdot (\mathbf{x}_2 \times \mathbf{x}_3)}, \qquad \psi_2(\mathbf{x}) = -\frac{\mathbf{x} \cdot (\mathbf{x}_1 \times \mathbf{x}_3)}{\mathbf{x}_1 \cdot (\mathbf{x}_2 \times \mathbf{x}_3)},$$

$$\psi_3(\mathbf{x}) = \frac{\mathbf{x} \cdot (\mathbf{x}_1 \times \mathbf{x}_2)}{\mathbf{x}_1 \cdot (\mathbf{x}_2 \times \mathbf{x}_3)}, \tag{A3}$$

and finally we can write (A3) as

$$\psi_i(\mathbf{x}) = \frac{\mathbf{x} \cdot (\mathbf{x}_j \times \mathbf{x}_k)}{\mathbf{x}_i \cdot (\mathbf{x}_j \times \mathbf{x}_k)}, \tag{A4}$$

where the following identities have been used:

$$(\mathbf{x}_i \times \mathbf{x}_j) = -(\mathbf{x}_j \times \mathbf{x}_i) \quad \text{and}$$

$$\mathbf{x}_i \cdot (\mathbf{x}_j \times \mathbf{x}_k) = \mathbf{x}_j \cdot (\mathbf{x}_k \times \mathbf{x}_i) = \mathbf{x}_k \cdot (\mathbf{x}_i \times \mathbf{x}_j).$$

From (A31)

$$\psi_i(\mathbf{x}_i) = \frac{\mathbf{x}_i \cdot (\mathbf{x}_j \times \mathbf{x}_k)}{\mathbf{x}_i \cdot (\mathbf{x}_j \times \mathbf{x}_k)} = 1$$

$$\psi_i(\mathbf{x}_j) = \frac{\mathbf{x}_j \cdot (\mathbf{x}_j \times \mathbf{x}_k)}{\mathbf{x}_i \cdot (\mathbf{x}_j \times \mathbf{x}_k)} = \frac{\mathbf{x}_k \cdot (\mathbf{x}_j \times \mathbf{x}_j)}{\mathbf{x}_i \cdot (\mathbf{x}_j \times \mathbf{x}_k)} = 0$$

$$\psi_i(\mathbf{x}_k) = \frac{\mathbf{x}_k \cdot (\mathbf{x}_j \times \mathbf{x}_k)}{\mathbf{x}_i \cdot (\mathbf{x}_j \times \mathbf{x}_k)} = \frac{\mathbf{x}_j \cdot (\mathbf{x}_k \times \mathbf{x}_k)}{\mathbf{x}_i \cdot (\mathbf{x}_j \times \mathbf{x}_k)} = 0.$$

Q.E.D.

Theorem 2. Furthermore, the basis functions (A1) satisfy the relation for a monotonic interpolant

$$\sum_{i=1}^{3} \psi_i(\mathbf{x}) = 1 \quad \forall \mathbf{x} \in \mathbf{T}_{1,2,3},$$

where $\mathbf{T}_{1,2,3}$ represents the triangle composed of the vertices $(\mathbf{x}_1, \mathbf{x}_2, \mathbf{x}_3)$.

Proof. Taking the sum of the basis functions in (A3) and using the identity $(\mathbf{x}_i \times \mathbf{x}_i) = 0$ gives

$$\sum_{i=1}^{3} \psi_i(\mathbf{x}) = \frac{\mathbf{x}\cdot[(\mathbf{x}_2\times\mathbf{x}_3)-(\mathbf{x}_2\times\mathbf{x}_1)-(\mathbf{x}_1\times\mathbf{x}_3)+(\mathbf{x}_1\times\mathbf{x}_1)]}{\mathbf{x}_1\cdot(\mathbf{x}_2\times\mathbf{x}_3)}. \tag{A5}$$

The numerator of (A5) can now be factored to yield

$$\sum_{i=1}^{3} \psi_i(\mathbf{x}) = \frac{\mathbf{x}\cdot[(\mathbf{x}_2-\mathbf{x}_1)\times(\mathbf{x}_3-\mathbf{x}_1)]}{\mathbf{x}_1\cdot(\mathbf{x}_2\times\mathbf{x}_3)}.$$

The denominator can be handled in a similar fashion to yield

$$\sum_{i=1}^{3} \psi_i(\mathbf{x}) = \frac{\mathbf{x}\cdot[(\mathbf{x}_2-\mathbf{x}_1)\times(\mathbf{x}_3-\mathbf{x}_1)]}{\mathbf{x}_1\cdot[(\mathbf{x}_2-\mathbf{x}_1)\times(\mathbf{x}_3-\mathbf{x}_1)]}, \tag{A6}$$

where the identity

$$\mathbf{x}_i\cdot(\mathbf{x}_j\times\mathbf{x}_i) = \mathbf{x}_j\cdot(\mathbf{x}_i\times\mathbf{x}_i) = 0$$

has been used. The terms inside the brackets of (A6) are exactly the components of the normal vector to the triangle $(\mathbf{x}_1, \mathbf{x}_2, \mathbf{x}_3)$. In other words

$$\mathbf{N} = (\mathbf{x}_2-\mathbf{x}_1)\times(\mathbf{x}_3-\mathbf{x}_1).$$

From the definition of the plane defined by this triangle which is

$$\mathbf{N}\cdot(\mathbf{x}-\mathbf{x}_1) = 0$$

we get

$$\mathbf{x}\cdot\mathbf{N} = \mathbf{x}_1\cdot\mathbf{N},$$

which gives for (A6)

$$\sum_{i=1}^{3} \psi_i(\mathbf{x}) = \frac{\mathbf{x}\cdot\mathbf{N}}{\mathbf{x}_1\cdot\mathbf{N}} = 1.$$

Q.E.D.

Theorem 3. The integral of any combination of the basis functions $\psi_i(\mathbf{x})$ within each triangle can be given in closed form as follows:

$$\int \psi_1^\alpha\psi_2^\beta\psi_3^\gamma\, d\Omega = \frac{\text{deter}\,\Delta\alpha!\beta!\gamma!}{(\alpha+\beta+\gamma+2)!}, \tag{A7}$$

where

$$\text{deter}\,\Delta = \begin{vmatrix} x_1 & x_2 & x_3 \\ y_1 & y_2 & y_3 \\ z_1 & z_2 & z_3 \end{vmatrix}. \tag{A8}$$

Proof. From (A2), the mapping from $(x, y, z) \to (\psi_1, \psi_2, \psi_3)$ is

$$\begin{bmatrix} dx \\ dy \\ dz \end{bmatrix} = \begin{bmatrix} x_1 & x_2 & x_3 \\ y_1 & y_2 & y_3 \\ z_1 & z_2 & z_3 \end{bmatrix}\begin{bmatrix} d\psi_1 \\ d\psi_2 \\ d\psi_3 \end{bmatrix}.$$

Let $\xi = \psi_1$, $\eta = \psi_2$ and from theorem 2,

$$\psi_3 = 1 - \psi_1 - \psi_2$$

and so $\psi_3 = 1 - \xi - \eta$. Therefore, the integral becomes

$$\int_{\Omega(x,y,z)} \psi_1^\alpha\psi_2^\beta\psi_3^\gamma\, d\Omega = \text{deter}\,\Delta\int_0^1 \xi^\alpha\left[\int_0^{1-\xi}\eta^\beta(1-\xi-\eta)^\gamma\, d\eta\right] d\xi,$$

which gives for the first integral in brackets by virtue of integration by parts

$$\int_0^{1-\xi}\eta^\beta(1-\xi-\eta)^\gamma\, d\eta = \frac{\gamma!}{(\beta+1)(\beta+2)\cdots(\beta+\gamma+1)}(1-\xi)^{\beta+\gamma+1},$$

but by completing the factorial in the denominater, we get

$$\int_0^{1-\xi}\eta^\beta(1-\xi-\eta)^\gamma\, d\eta = \frac{\beta!\gamma!}{(\beta+\gamma+1)!}(1-\xi)^{\beta+\gamma+1}.$$

Integrating the remaing terms, we get

$$\int_{\Omega(x,y,z)} \psi_1^\alpha\psi_2^\beta\psi_3^\gamma\, d\Omega = \frac{\text{deter}\,\Delta\beta!\gamma!(\beta+\gamma+1)!}{(\beta+\gamma+1)!(\alpha+1)(\alpha+2)\cdots(\alpha+\beta+\gamma+2)},$$

and simplifying and completing the factorial yields

$$\int_{\Omega(x,y,z)} \psi_1^\alpha\psi_2^\beta\psi_3^\gamma\, d\Omega = \frac{\text{deter}\,\Delta\alpha!\beta!\gamma!}{(\alpha+\beta+\gamma+2)!}.$$

Q.E.D.

REFERENCES

Côté, J., 1988: A Lagrange multiplier approach for the metric terms of semi-Lagrangian models on the sphere. *Quart. J. Roy. Meteor. Soc.,* **114,** 1347–1352.

Giraldo, F. X., 1997: Lagrange–Galerkin methods on spherical geodesic grids. *J. Comput. Phys.,* **136,** 197–217.

Le Roux, D. Y., C. A. Lin, and A. Staniforth, 1997: An accurate interpolating scheme for semi-Lagrangian advection on an unstructured mesh for ocean modelling. *Tellus,* **49A,** 119–138.

McDonald, A., and J. R. Bates, 1989: Semi-Lagrangian integration of a gridpoint shallow water model on the sphere. *Mon. Wea. Rev.,* **117,** 130–137.

McGregor, J. L., 1993: Economical determination of departure points for semi-Lagrangian models. *Mon. Wea. Rev.,* **121,** 221–230.

Ritchie, H., 1987: Semi-Lagrangian advection on a Gaussian grid. *Mon. Wea. Rev.,* **115,** 608–619.

Silvester, P., 1969: High-order polynomial triangular finite elements for potential problems. *Int. J. Eng. Sci.,* **7,** 849–861.

Williamson, D. L., J. B. Drake, J. J. Hack, R. Jakob, and P. N. Swarztrauber, 1992: A standard test set for numerical approximations to the shallow water equations in spherical geometry. *J. Comput. Phys.,* **102,** 211–224.